Deliverable

D6.5 Report on the Development of RLA, EEW and OEF at European Scale

Deliverable information	
Work package	WP6. Demonstration: Pilot and demonstration sites for RISE technologies and methods
Lead	EUCE
Authors	Helen Crowley, EUCE Jamal Dabbeek, EUCE Sevgi Ozcebe, EUCE Remy Bossu, EMSC Francesco Finazzi, UniBG Carlo Cauzzi, ETH Laurentiu Danciu, ETH Athanasios Papadopoulos, ETH Marta Han, ETH Leila Mizrahi, ETH Alberto Michelini, INGV Licia Faenza, INGV Valentino Lauciani, INGV
Reviewers	Ian Main, UEDIN
Approval	Management Board
Status	Final
Dissemination level	Public
Delivery deadline	28.02.2023
Submission date	28.02.2023
Intranet path	DOCUMENTS/DELIVERABLES/Deliverable_6.5.pdf

This project has received funding from the European Union's Horizon 2020 research and innovation programme under grant agreement No 821115

Table of Contents

Summary

This deliverable includes a summary of the advances that have been made in the RISE project towards European services for Rapid earthquake Loss Assessment (RLA), crowd-sourcing based Earthquake Early Warning (EEW) and Operational Earthquake Forecasting (OEF).

1. Introduction

This deliverable aims to bring together and summarise the advances that have been made in the RISE project towards European services for Rapid earthquake Loss Assessment (RLA), crowd-sourcing based Earthquake Early Warning (EEW) and Operational Earthquake Forecasting (OEF). The first two include the most advanced services, and have components that are already operating at the European scale, such as the European ShakeMap system and the Earthquake Network (EQN) smartphone app. Both services were fully operational during the recent sequence of earthquakes that struck eastern Turkey and Syria on 6th February 2023, first with a Mw 7.8 shock, then followed only hours later by a second Mw 7.6 event.

The wider issues related to communication of the results of such European services are not dealt with herein, and have instead been investigated further in WP5. The focus of this deliverable is on the feasibility of these European services in terms of technical capabilities.

2. European Rapid Loss Assessment (RLA) System

When an earthquake occurs, there are many remote sensors that record data from the event: waveforms recorded by seismic instruments are used to locate the hypocentre and magnitude of the earthquake and to assess the strong ground shaking at the surface of the earth; people and buildings feel the shaking and observe or record the impact that it has on them. All of these data can be used to rapidly estimate, in the minutes, hours or days following an earthquake, the impact that the earthquake has on the surrounding people, buildings and infrastructure. In the first few minutes following an earthquake, a simple qualitative assessment (e.g., no impact, minor impact, major impact) is often sufficient to understand the magnitude of the event, and this is referred to as Rapid Impact Assessment In the following hours, however, it becomes important to understand the impact in terms of quantitative losses (e.g., number of collapsed buildings, number of fatalities or homeless people, direct economic loss) and this estimation is referred to as Rapid Loss Assessment. This fast assessment of the impact of the earthquake provides first order estimates of the losses which can be continually updated as more information and data arrive from the remote sensors.

It can often take days or even months for the true toll of an earthquake to be measured and reported. Stakeholders such as early responders, governments, and the insurance industry all need to have an estimate of the potential magnitude of the losses much earlier than this, so that they can plan and better manage the recovery phase after the earthquake. For example:

- Early responders such as civil protection agencies need to know which areas have been most hit, and the scale of collapsed buildings, so that they can send the right teams and equipment to search for trapped survivors. They will also need an estimate of the number of homeless people, so they can prepare emergency shelter.
- Governments may need to allocate funding for the rescue and recovery efforts, either nationally or as part of international aid, when the event has occurred in another country.
- Insurers need to plan for post-earthquake damage assessments to manage the potential insurance claims (e.g., Pittore et al., 2015).

Whilst these initial rapid estimates of loss are statistical (i.e., they can only provide a distribution of the expected damage and loss, rather than identify specific buildings that will be damaged) and they contain a number of uncertainties, they nevertheless provide useful, actionable information for these communities.

2.1 European ShakeMap System

For over 13 years, the U.S. Geological Survey (USGS) has been running a global rapid loss assessment service called PAGER[1] (Prompt Assessment of Global Earthquakes for Response (Earle et al., 2009), that makes use of ShakeMap (Wald et al., 1999). ShakeMap provides an estimate of ground shaking in the area struck by an earthquake. An earthquake with a specific magnitude, location and depth will produce a range of ground shaking levels at sites throughout the region depending on distance from the earthquake, the local site conditions, and variations in the propagation of seismic waves from the earthquake, due to complexities in the structure of the Earth's crust. Ground shaking levels can be represented through macroseismic intensity, which is a description of the effect of the earthquake on people and structures (e.g., Grünthal, 1998), or through measured shaking parameters, such as the peak acceleration of the ground recorded by an accelerograph. Following an earthquake, data on the ground shaking from both observations of macroseismic intensity and recordings from seismic instruments are automatically processed and distributed via dedicated software and web services, without the need for any human intervention. These data are combined with empirical ground motion models (applied to the areas without any data), to produce maps of likely ground shaking. The accuracy of the resulting ShakeMap will depends on the density of the observations and on the faithfulness of the ground motions model(s) to represent the ground motion where no observations are present.

Within RISE, a European ShakeMap service prototype (http://shakemapeu.ingv.it) using the latest version of ShakeMap (v4, Worden et al., 2020) has been consolidated under the management and maintenance of both ETH Zurich and the National Institute for Geophysics and Volcanology in Italy (INGV) (Fig. 1). The service adopts the publicly available ShakeMap (v4) web portal development (Jozinovič et al., 2022) to display all the ShakeMaps and making available the resulting metadata. A number of web services produced by EMSC (the European-Mediterranean Seismological Centre: https://www.emsc-csem.org) and ORFEUS (Observatories and Research Facilities for European Seismology: https://www.orfeus-eu.org/) are used by the European ShakeMap system to automatically register when an earthquake above magnitude 3.5 occurs within Europe, and to receive any recorded strong motion data.

The European ShakeMap adopts Docker containers (Merkel, 2014) for the ShakeMap v4 software and, for map revision and software parameters configuration changes, a scheme based on git (https://github.com/) has been devised. This allows for the preservation of access security to the portal and optimal interaction by the scientists and the staff. In practice, if an earthquake occurs and an authorised user wants to manually add new data or, for a large event, the fault geometry, (s)he can just add the new files in the event directory on the dedicated github directory and git itself will trigger the run of the new updated ShakeMap. In this scheme, every time that a new ShakeMap is generated, an email is sent to the group of maintainers containing the links to the event GitHub directory where the input data can be possibly be modified. At the same time, this scheme preserves the entire log of the analysis performed easing very much the reproducibility of the results. This greatly simplifies the revision and maintenance process by possibly a large pool of people located in different countries.

The European ShakeMap system is fully consistent with the data and modelling protocols used in the national services for Italy, Greece and Switzerland (and also therefore could serve as a backup for these national installations), and there are plans to expand this harmonisation to other European countries.

Felt reports have been collected by the EMSC in large numbers since 2013 (Bossu et al., 2018). They differ from online macroseismic data such as DYFI (USGS) (Wald et al., 2011) by replacing the online questionnaire by a set of cartoons depicting different shaking and damage levels (Fig. 2). The intensity value is assigned by the user choosing the cartoon appropriate to their situation.

---

[1] https://earthquake.usgs.gov/data/pager/

Cartoons make global collection of eyewitness reports easier and faster. The median collection time in 2022 was about 10 min for 250,000 collected reports (see Fig. 3). Geographical coverage was significant with 75 countries giving at least 1,000 collected reports. The USGS has developed a method to ingest the EMSC felt reports in their global ShakeMaps based on the same methodology as that used for DYFI ingestion (Quitoriano and Wald, 2022). It has been shown to significantly reduce the uncertainty of rapid impact assessment derived from ShakeMaps. The software is freely available. So far, felt reports have been distributed by webservices for research purposes. Their ingestion in Shakemaps requires a different mechanism. EMSC is currently testing a messaging system named HMB to share them in real time with USGS. Similar tests should be performed soon with several national institutes in Europe as well as with the prototype European Shakemap service. 2023 should see the first use of EMSC felt reports in ShakeMaps in operational conditions.

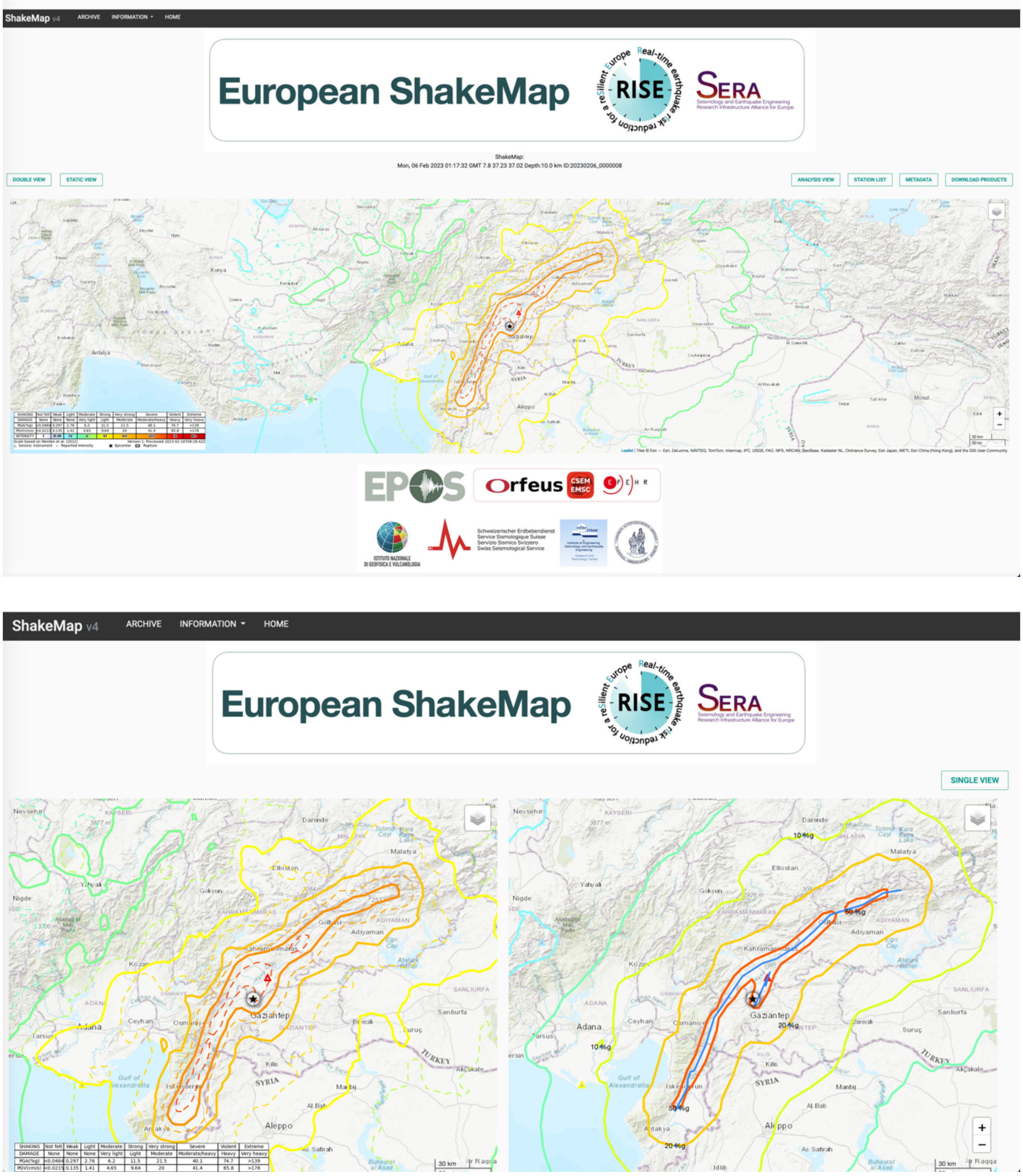

Fig. 1 European ShakeMap Service: http://shakemapeu.ingv.it/. The source code for this web portal is publicly available at: https://github.com/INGV/shakemap4-web. The top image shows the ShakeMap (macroseismic intensity) for the 6th February mainshock in eastern Turkey, whereas the bottom image shows the double view comparing the macroseismic intensity map with the PGA map (also showing the fault).

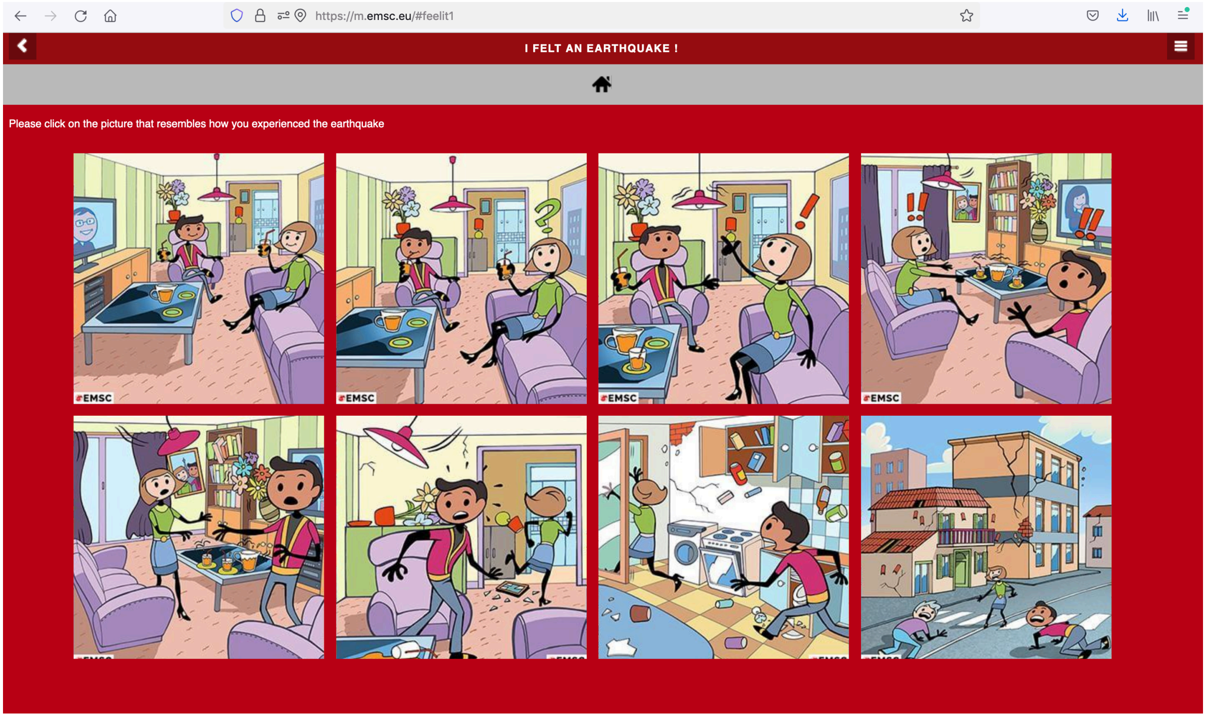

Please click on the picture that resembles how you experienced the earthquake

Fig. 2 EMSC's 'I felt an earthquake!' form for crowdsourcing felt data after an earthquake (https://m.emsc.eu/#feelit1)

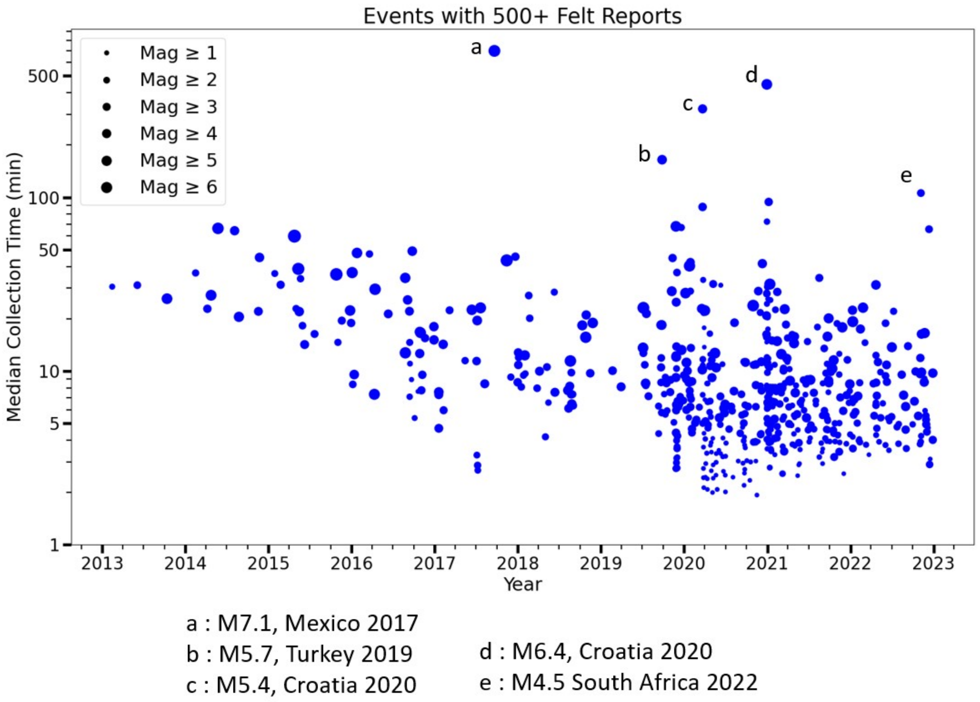

Fig. 3 Time evolution of the median collection time (logarithm scale) for earthquakes with at least 500 felt reports. The collection time had significantly decreased by 2019-2020 and remained reduced since. The outliers are events which have attracted media attention; they are typically of larger magnitude.

2.2 European Vulnerability and Exposure

The USGS's PAGER system uses global exposure and vulnerability models to assess the losses from earthquakes (e.g., Jaiswal and Wald, 2008, 2013; Jaiswal et al., 2009). An exposure model provides information about the spatial distribution of residential and non-residential building classes in terms of building count, area, occupants and replacement cost. Vulnerability models provide an estimation of damage to buildings and their contents under given levels of ground shaking, and the ensuing economic losses and loss of life.

In Europe, we make use of European exposure and vulnerability models that were initiated in the Horizon 2020 SERA project (http://www.sera-eu.org/en/home/) and have been completed in the RISE project, and made publicly available through the risk services of EFEHR (European Facilities for Earthquake Hazard and Risk: http://risk.efehr.org) (Crowley et al, 2021).

Exposure and vulnerability models for 44 European countries are available at the following repository: https://gitlab.seismo.ethz.ch/efehr/esrm20. For detailed scenario damage and loss modelling, as carried out in Rapid earthquake Loss Assessment, it is fundamental to use a higher resolution of the exposure models that those used in the European seismic risk model, such that a more detailed representation of the impacts can be estimated and mapped.

The exposure models used in ESRM20 have now been disaggregated to a 30 arcsecond grid using WorldPop[2], using openly available tools developed in the RISE project in collaboration with the GEM Foundation[3] (Dabbeek et al., 2021) and they have been added to the aforementioned ESRM20 repository. Fig. 4 and Fig. 5 below show a comparison of the original resolution of the ESRM20 residential exposure models in the south-eastern area of Europe (with the coordinates of the locations of the exposure in each administrative region shown in red) with the disaggregated 30 arcsecond exposure models.

Fig. 4 Original resolution of the residential building stock exposure models in south-eastern Europe

---

[2] https://www.worldpop.org/

[3] https://github.com/GEMScienceTools/spatial-disaggregation

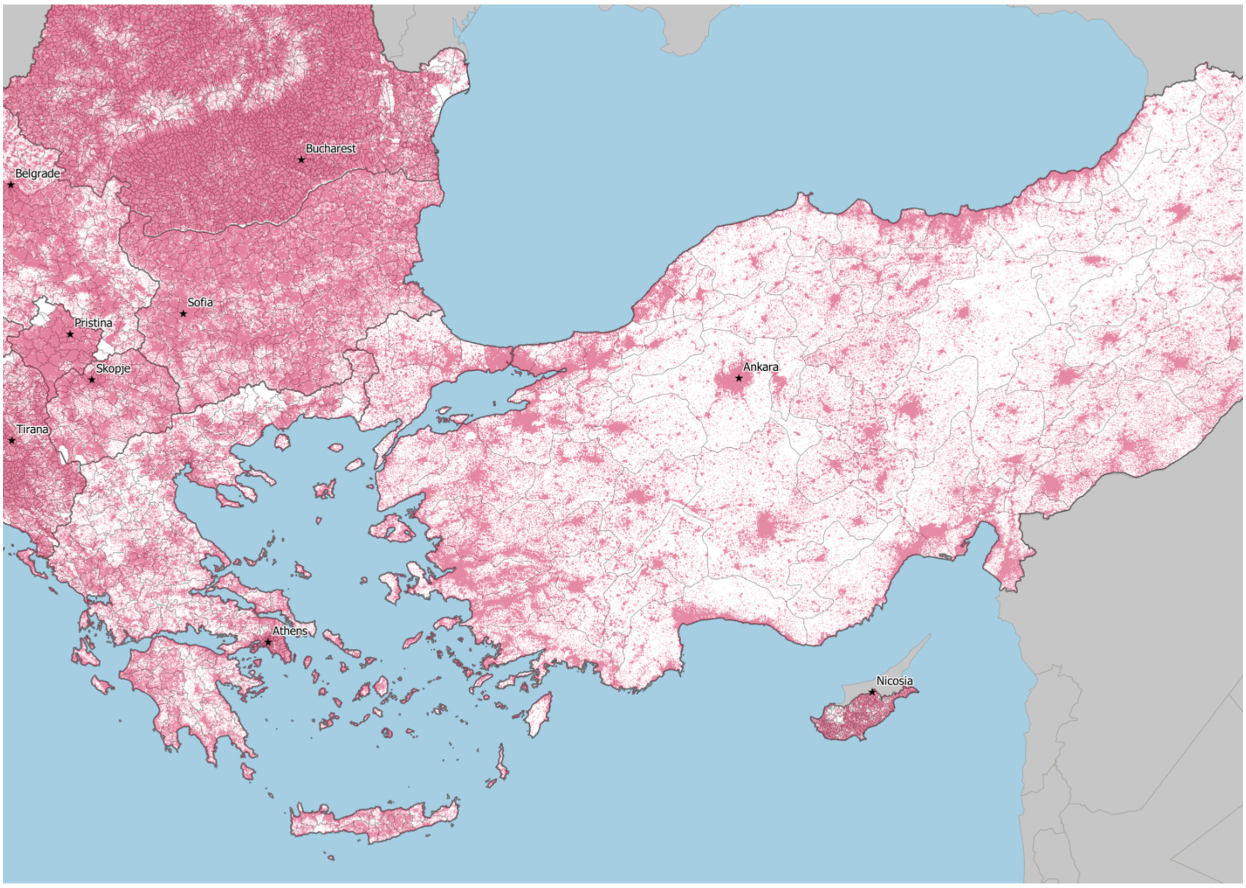

Fig. 5 30 arcsecond disaggregated exposure models developed in the RISE project

Furthermore, for the development of the demonstration activities described in Deliverable D6.1, the vulnerability models have been expanded to include injuries for four different severity levels (as defined in HAZUS – FEMA, 2003). These models are now included in the European vulnerability repository: https://gitlab.seismo.ethz.ch/efehr/esrm20_vulnerability.

2.3 European Rapid earthquake Loss Assessment Software

The exposure and vulnerability models have been formatted as input files for the OpenQuake-engine, an open source software for seismic hazard and risk assessment (https://github.com/gem/oq-engine), and can be used in the workflow shown in Fig. 6 to produce damage and loss statistics and maps, once the appropriate ShakeMap data (i.e., grid and uncertainty xml files) have been downloaded from the European ShakeMap service using the available webservices.

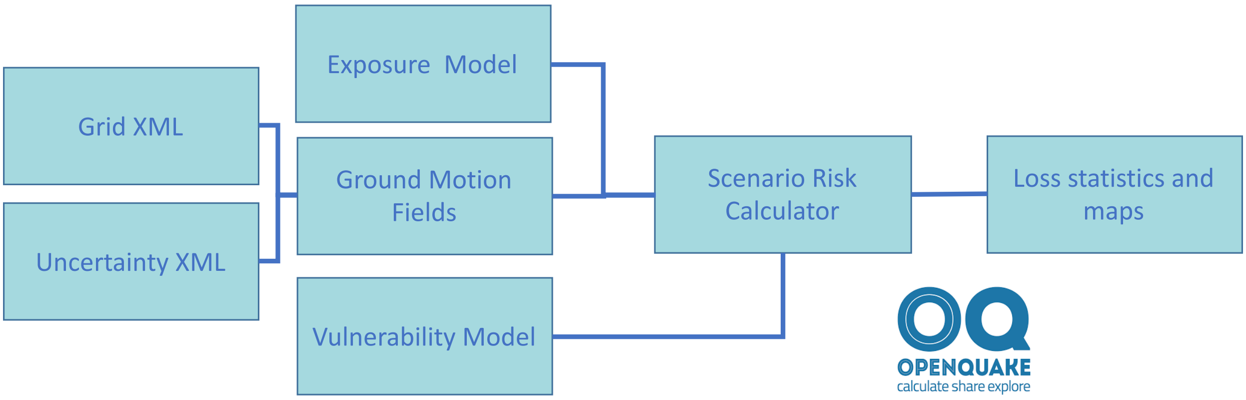

Fig. 6 Scenario from ShakeMap workflow of the OpenQuake engine (Pagani et al 2014)

A first version demonstrator of the ESRM20 Rapid earthquake Loss Assessment service has been openly published on a GitLab repository[4]. This demonstrator uses web services to download ShakeMaps as soon as they have been published on the European ShakeMap system, retrieves and crops the 30 arc second resolution exposure models for the countries covered by the ShakeMap grid, and launches the scenario damage and risk calculations with the OpenQuake-engine. Currently the code is set up to calculate completely damaged buildings, economic loss and fatalities, but it can be easily expanded to output other damage states as well as injuries (using the newly developed injury models described above). An example output of the service (in terms of the loss distribution for Turkey and Greece for the 30th October 2020 Samos/Izmir earthquake) is shown in Fig. 7. The mean, median and fractiles of loss can be extracted from these distributions.

These distributions are plotted using the impact scale proposed for PAGER by Wald et al. (2010). The alert colour assigned to the event in PAGER is given by the median economic loss estimate for the whole event. The ReLA software is instead set up to produce the same type of distributions as PAGER, but the alert is currently provided for each metric and country separately based on the median value in the plots in Fig. 7; there would thus be an orange alert for fatalities in Turkey, but yellow in Greece, and there would be an orange alert for economic loss in Turkey, but yellow in Greece. Maps of the spatial distribution of losses can also be produced with the tool, as shown in Fig. 8. These have been produced with a modified version of the impact scale, given that the losses within each 30 arc second grid cell will be much lower than the aggregate losses for the event. These maps can help quickly identify the areas that have been most highly impacted by the event.

The ESRM20 Rapid earthquake Loss Assessment (ReLA) code has been applied to all events in the European ShakeMap archive since it was launched in 2020 (which at the time of producing this deliverable was a total of 1100 events with magnitude above 4). The results provided in terms of median fatalities are compared with the observed losses reported in EM-DAT in Fig. 9; the confusion matrix shows that the alert level would have been correctly estimated in 98.6% of the cases (and overestimated by one alert level in 1.4%). Similar plots, for 10 years worth of events, were recently produced by the USGS for the PAGER system (Wald et al., 2022).

Reasons for the overestimation in 1.4% of the cases are being investigated and these activities will continue beyond the project (and any modifications will be incorporated as part of the European earthquake scenario and loss modelling services currently offered through EPOS/EFEHR and those being developed in the Geo-INQUIRE project).

The current hypothesis is that a new scenario loss modelling workflow, very recently implemented in v3.16 of the OpenQuake-engine (see https://github.com/gem/oq-engine/issues/8317), will bring further improvements. In this workflow, rather than download the grid and uncertainty xml files from the European ShakeMap system (see Fig. 5), only the earthquake data (epicentre and magnitude), the fault and the stations data in JSON format are downloaded from the European ShakeMap system.

The OpenQuake-engine then calculates multiple ground motion fields using the same conditional multivariate normal (MVN) approach recently developed by Engler et al. (2022). The advantage of this approach is that alternative ground motion models can be explored (and the one with the lowest bias can be selected), limits on the sampled ground motion values can be implemented (it is noted that the current calculator does not truncate the sigma in the ground motion models, and thus extremely large ground motion values can be sampled), and additional station data (which might be available but are not integrated in the European ShakeMap system) can be accounted for.

---

[4] https://gitlab.seismo.ethz.ch/hcrowley/rapid_loss_eu

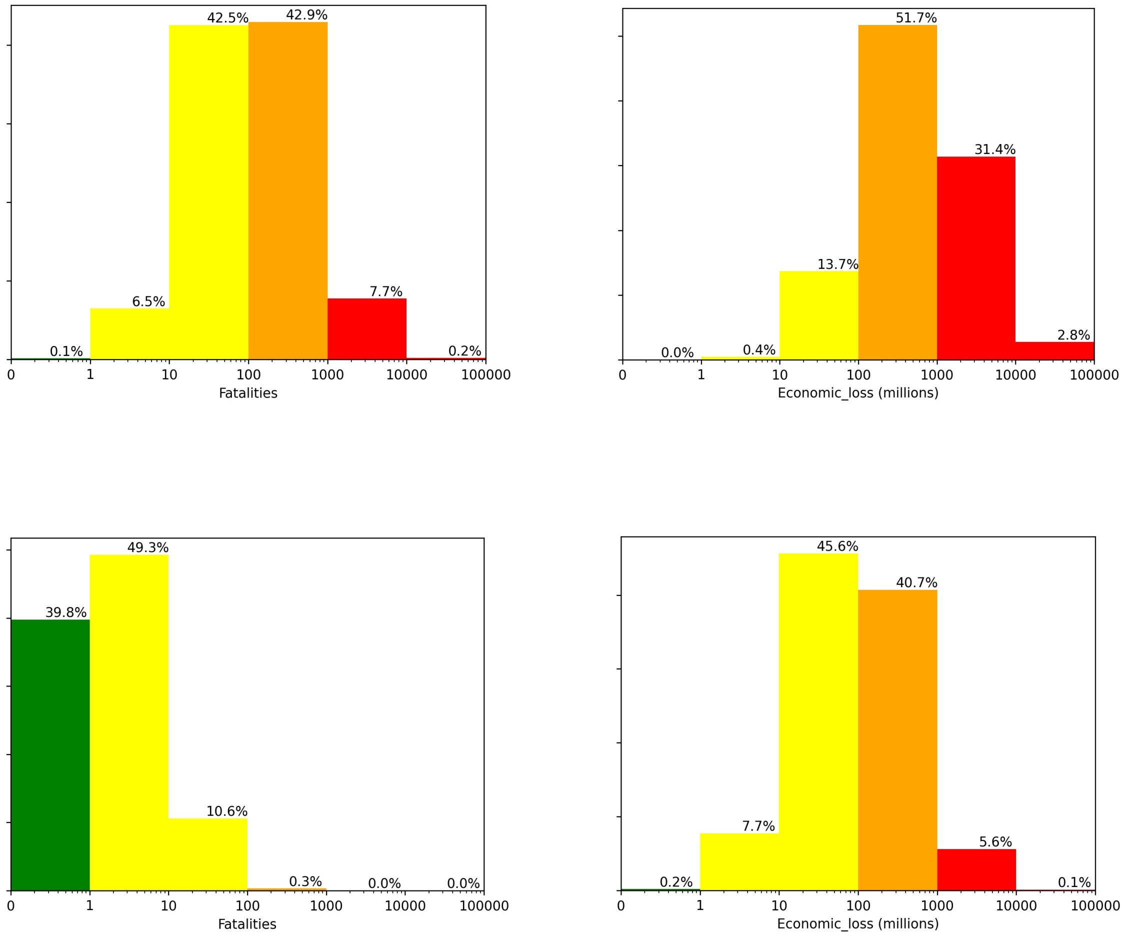

Fig. 7 ***Example output for the 30th October 2020 Samos/Izmir earthquake. Distribution of the fatalities (left) and economic loss (right) for (top) Turkey and (bottom) Greece based on the PAGER impact scale (Wald et al., 2010)***

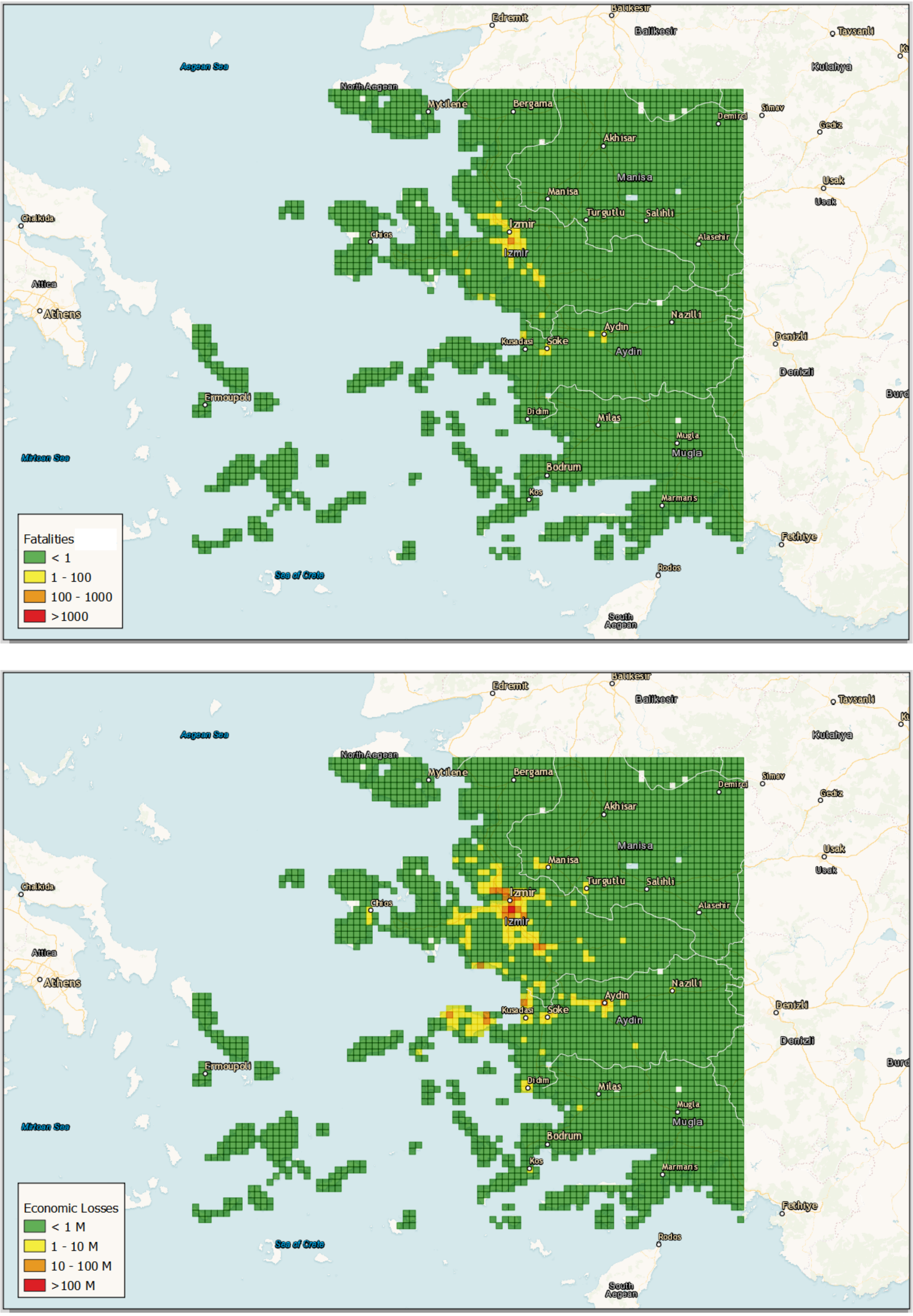

Fig. 8 Spatial distribution of fatalities (top) and economic losses (bottom) on a 30 arc second grid, using a modified version of the PAGER impact scale

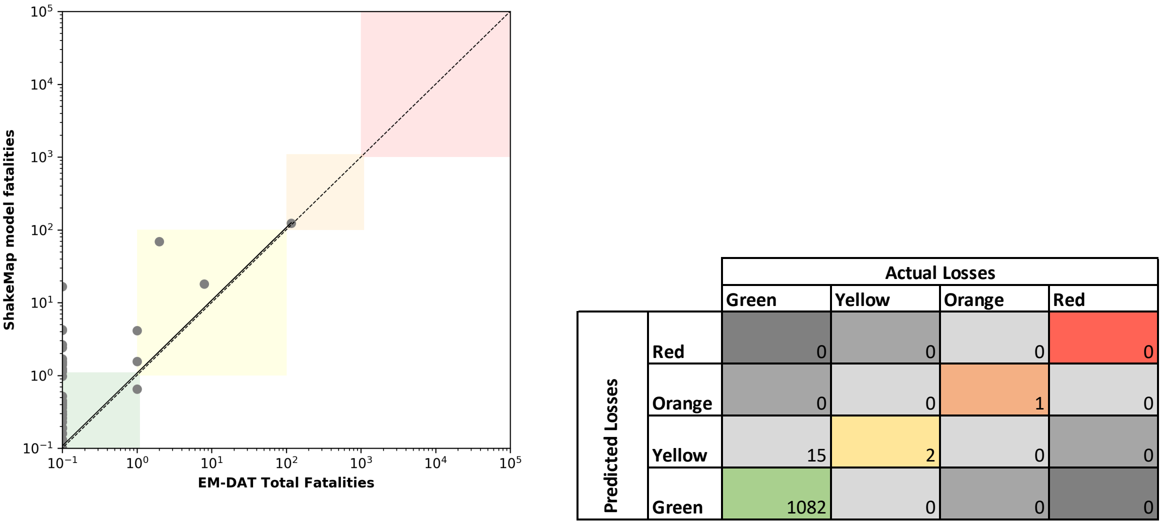

		Actual Losses			
		Green	Yellow	Orange	Red
Predicted Losses	Red	0	0	0	0
	Orange	0	0	1	0
	Yellow	15	2	0	0
	Green	1082	0	0	0

Fig. 9 ***(Left) Estimated median fatalities using the ESRM20 Rapid earthquake Loss Assessment (ReLA) code*** **(https://gitlab.seismo.ethz.ch/hcrowley/rapid_loss_eu)** ***for all earthquakes in the European ShakeMap archive since 2020*** **(http://shakemapeu.ingv.it/archive.html)** ***compared with the reported losses in EMDAT*** **(www.emdat.be)*****. (Right) Confusion matrix showing the number of events for which the ESRM20 ReLA fatality-based alerts were correct, or over/underestimated (grey cells).***

3. European Crowdsourcing-based Earthquake Early Warning (EEW)

3.1 The Earthquake Network citizen science initiative

Started in 2012, Earthquake Network (EQN) is a citizen science initiative implementing the first smartphone-based earthquake early warning (EEW) system. Thanks to a smartphone app, the devices made available by citizens are exploited to create a network for the real-time detection of earthquakes. When an earthquake is detected, an alert is sent to the smartphones with the app installed and published on social networks (Twitter and Facebook) and on Telegram channels. The aims of EQN are to possibly alert people before strong ground shaking begins and to improve people's awareness of the seismic events that are happening in their area.

The RISE and the TURNkey H2020 projects have been the opportunity for EQN to be studied in detail by seismologists and scientists. The main findings are summarised here, while the details are given in RISE Deliverable 5.9 and in the cited scientific articles.

3.1.1 EQN detection capabilities

Using a probabilistic model, Finazzi et al. (2022) showed that the detection capability of the EQN smartphone network is mainly affected by the number of smartphones in the clusters which compose the network and by the shaking intensity at the nearest cluster from the epicentre. For high intensities, the probability of detection in practically one regardless of the number of smartphones in the nearest cluster, suggesting that EQN is suitable for EEW services, where the focus is on strong and potentially dangerous earthquakes.

3.1.2 EQN detection delay

From the analysis of the EQN detection logs, Bossu et al. (2022) showed that the EQN detection delay is again related to the smartphone network geometry. In countries where the EQN smartphone app is popular, like Chile, Italy and the U.S., the EQN detection delay is comparable to the delay of EEW systems based on scientific-grade instruments such as ShakeAlert.

3.1.3 EQN warning time

In Bossu et al. (2022), warning times have been computed for 53 EQN detections related to earthquakes with magnitude higher than 4.5 and for some target shaking intensities. It has been discovered that, in at least two cases, EQN alerted people exposed to intensity 6 shaking with warning times up to 7 seconds. In all other cases, warning times have been as high as 100 seconds for people exposed to intensity 4 and 5. This proved that EQN routinely provides EEW services to its participants and to people following EQN on Twitter or Telegram.

3.1.4 EQN's participant reactions to EEW

In Fallou et al. (2022), results from a quantitative survey have been analysed to understand how EQN services are perceived by EQN participants and to understand how they react when a warning is received on the smartphone. Specifically, the survey targeted participants who experienced the M8.0 earthquake that hit central Peru on May 26th, 2019. The most relevant finding is that only 34.7% of the participants who received the alert before the shaking reacted by moving to a safe place or by running outside the building. Most of the participants spent the time between the alert and the shaking warning their relatives, either nearby or on social media.

3.1.5 EQN's performance during the Turkish-Syrian of February 6, 2023

The recent Turkish-Syrian earthquake of February 6, 2023 has been detected by the EQN system with a delay of only 11 seconds from origin time. This allowed to disseminate a rapid alert to people exposed to very damaging shaking levels. While the data analysis is still ongoing, preliminary results suggest that EQN provided a forewarning up to 25 seconds for people exposed to shaking intensities between 8.5 and 9.

4. European Operational Earthquake Forecasting (OEF)

The goal of operational earthquake forecasting (OEF) is to provide reliable, up-to-date information about the likelihood of earthquakes (and potentially also their impacts in terms of ground shaking, damage and losses) in a given area. By combining the latest data and modelling techniques, the aim is to better understand the patterns and processes behind earthquakes, leading to more accurate and actionable information for decision-makers. With continued progress and refinement, these efforts can help to minimize the impact of earthquakes on communities and reduce the risks associated with seismic activity.

The feasibility of setting up a European OEF service - from rates, to ground motion to damage and losses – has been explored in the RISE project. Whilst such a model cannot yet be demonstrated at the European scale, we provide here a summary of the steps that have been taken towards achieving such a goal and the main challenges and areas of future development that are still needed, and that are planned in upcoming projects, such as GeoINQUIRE.

4.1 A European Operational Earthquake Forecast Model – Occurrence Rates

Operational Earthquake Forecasting (OEF) is an evolving effort that has seen significant progress in recent years in several countries, including New Zealand (Christophersen et al., 2017), the USA (Field et al., 2017; T. Jordan et al., 2011; T. H. Jordan et al., 2014), Italy (Marzocchi et al., 2014; Marzocchi and Lombardi, 2009), and others. Within the RISE project, a forecasting model has also been developed and tested at SED for Switzerland (Mizrahi et al., 2023) and a system which operationally produces forecasts is in development.

A forecasting model similar to the one of Mizrahi et al. (2023) has been developed within RISE for Europe (Han et al., 2023). It is meant to be simple and serve as the basis for the development of future models. The goal of these efforts is to provide updated earthquake probabilities in real-time, relying on long-term seismicity rates (Danciu et al., 2021; 2022) as well as short-term clustering patterns to determine time-dependent earthquake rates. The IT setup of the Swiss OEF system will analogously be applied in the case of the pan-European model.

One of the models being most widely used for time-dependent earthquake forecasting is the Epidemic-Type Aftershock Sequence (ETAS) model (Ogata 1988). It models earthquake occurrence as a spatio-temporal self-exciting point process, using basic empirical laws such as the Omori-Utsu law for the temporal evolution of aftershock rate, the Gutenberg-Richter law to describe the size distribution of earthquakes, the exponential productivity law and the decay of the rate with increasing distance from the mainshock. ETAS separates earthquakes into background seismicity and aftershock clusters, and its main focus and core advantage over time-independent forecasting models lies in accurately modelling aftershock occurrence.

Our proposed ETAS model is calibrated on the European earthquake catalogue, which has been put together thanks to the efforts of ESHM20 (Danciu et al., 2021; 2022). The calibration was done using the Python code developed by Mizrahi et al. (2023), which can in principle be used to calibrate basic ETAS models on any given catalogue. However, adjustments are necessary in the case of a European ETAS model.

The data available for model training is highly inhomogeneous, as it covers a relatively large area, unequally covered by the seismic networks both in time and space. For instance, the completeness magnitude above which we observe all events that occur is above 6 for some regions and time periods, whereas for other regions and more recent time periods, it goes down to 3.5. Using the highest available M_C would result in losing a large amount of valuable data, while assuming a completeness level that is lower than the true one would introduce biases to our calculations. Another variability in the dataset comes from the precision at which the magnitudes are measured and the different magnitude types that are being used. Fig. 10a-b demonstrates the completeness magnitude changing with time, and the discretization of the data. The magnitude frequency distribution of the catalog is shown in Fig. 10c, and the spatial distribution of earthquakes in the training catalog is visualized in Fig. 10d.

The study of (Danciu et al., 2021; 2022) provides the expert evaluations of the completeness magnitudes by regions and time periods. Knowing these MC values allows us to account for the incompleteness of data during model calibration as described in (Mizrahi et al., 2021). Although more precise magnitude resolution is available for a part of the data, the agreed-on precision is 0.2, as in (Danciu et al., 2021; 2022). The fit of our proposed model to the training data is shown in Fig. 11, where it is also compared to ETAS models that were previously calibrated for Switzerland and California.

The model has been tested for consistency retrospectively using CSEP consistency tests (Savran et al., 2022; Schorlemmer et al., 2007; Rhoades et al., 2011; Zechar et al., 2010, see Fig. 12) and will be compared using pseudo-prospective tests to the time-independent rate forecast of (Danciu et al., 2021; 2022) and other ETAS variants that include additional information on the spatial distribution of background seismicity.

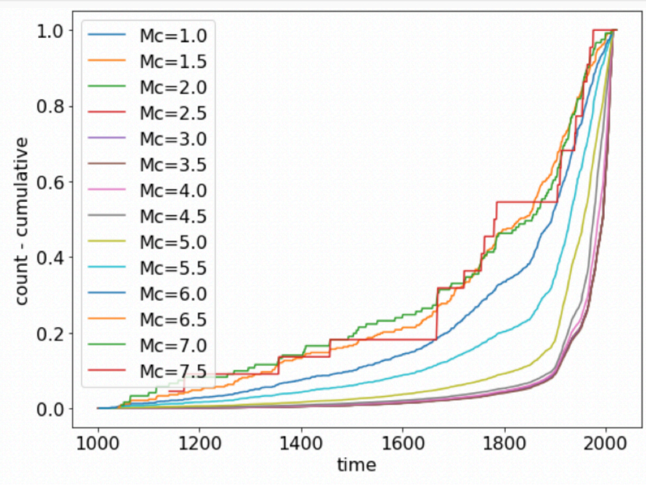

Fig. 10a Cumulative event count above M_C. If the catalog were complete at a given M_C, the cumulative event count would increase linearly. However, in the present catalog spanning the years 1000 to 2015, changes in the slope are evident for all tested values of M_C.

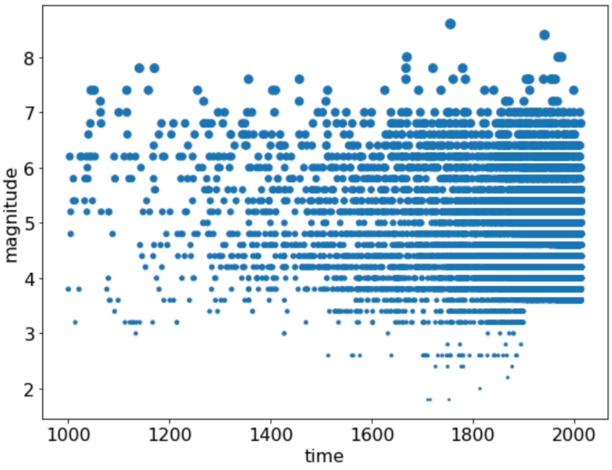

Fig. 10b The scatter plot of the event magnitudes through time. Incompleteness at lower magnitudes is evident, although the true M_C cannot be estimated just from this visualization. The discretization of the data is visible in the characteristic horizontal spacing between the dots.

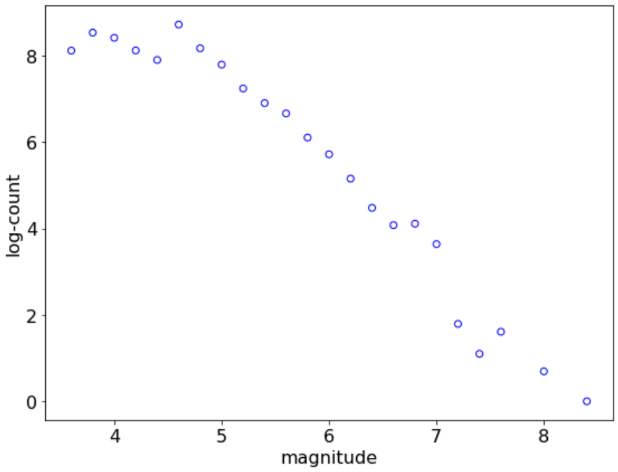

Fig. 10c The count of magnitude bins on log-scale. By Gutenberg-Richer law, the dots should be well fitted with a line. The data is filtered to only show events above the expert-given M_C. Incompleteness below M5.0 is due to differences in M_C by region.

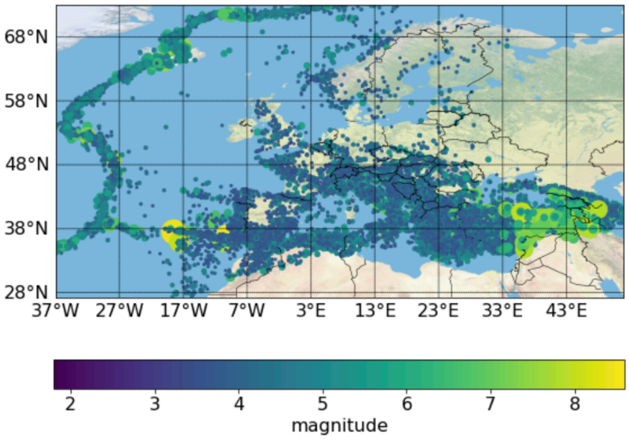

Fig. 10d Spatial distribution of the data. Dot size and color reflect the magnitude of the events.

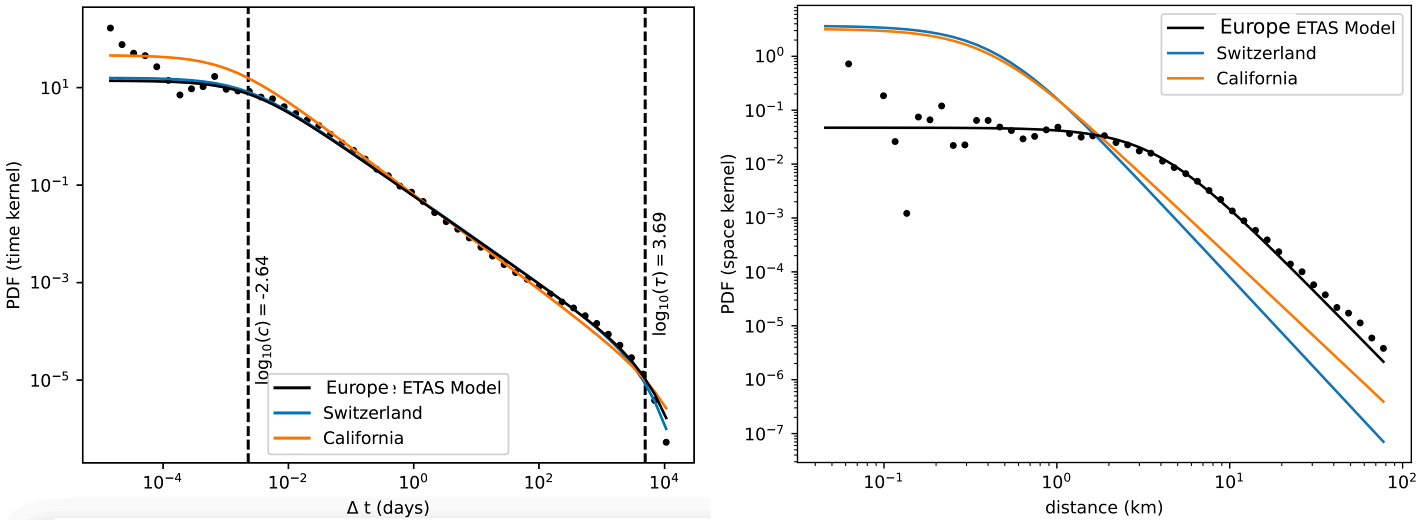

Fig. 11 The temporal and spatial decay inverted by the ETAS model. The lines show the theoretical decay based on our ETAS model, while the dots show the observed decay. The observed triggering is based on the branching structure also inverted by the model. Spatial kernel depends on the magnitude of the triggering event, here we show an example for M4.0.

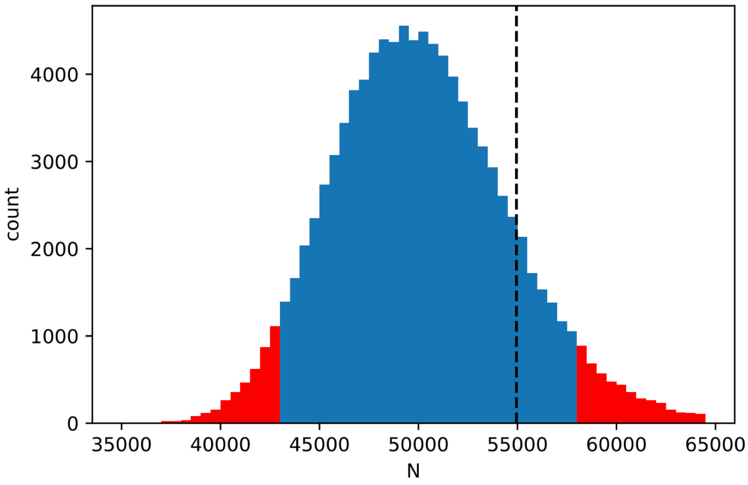

Fig. 12 One of the PyCSEP tests: N-test (number test). The histogram shows the counts of events in 100k simulated catalogs based on our ETAS model. The actual (observed) number of events is represented by the dashed line. The model passes the N-test with p-value around 0.3

4.2 A European OEF Model – Earthquake Ruptures and Ground Motion Modelling

Operational Earthquake Forecast (OEF) is typically underpinned by point processes like the ETAS model described in the previous section. The output of these models is typically a set of stochastic earthquake catalogues over the forecasting interval of interest. By performing statistics on these catalogues, the recurrence rate of earthquakes over the relevant time interval and possibly over different spatial and/or magnitude bins can be derived. This is the primary and most common product of OEF systems.

In most cases, the information contained in the simulated stochastic catalogues is limited to epicentral location and magnitude. While this is sufficient for estimating recurrence earthquake rates, additional source attributes are required for seismic hazard and/or risk analyses.

In order to extend the OEF beyond earthquake recurrence rates (or synthetic catalogues), and to assess the levels of ground shaking for each earthquake in the catalogue, and subsequently the damage and loss (see Section 4.3), it is necessary to translate the synthetic catalogues from effective two-dimensional point sources to three dimensional finite ruptures.

More precisely, the synthetic earthquake catalogues would need to be augmented with information such as the hypocentral depth and earthquake ruptures parameters such as strike, rake and dip. These are the minimal criteria for establishing the geometry of the finite ruptures that will be associated with each catalogued event. The finite ruptures can subsequently be used to derive source-to-site distances and other variables required for ground motion prediction modelling. This requires the integration of more information to constrain the scaling of the finite fault dimensions with magnitude, their depth in the Earth’s crust, their orientation, and their style-of-faulting.

Some forecasting models can provide directly some parameters (e.g. depth; Guo, Zhuang, and Zhou 2015) or the exact ruptures (Field et al. 2017). When this is not the case, the rupture parameters can be obtained or sampled from an underlying seismogenic source model.

In Deliverable D6.1 these issues have been explored further and there it is explained that a zonation of rupture property distributions across Europe would be required, which would divide Europe into specific zones (polygons) and provide for each zone the following information:

i) Magnitude to rupture area scaling relation,
ii) rupture aspect ratio (i.e., v=L/W),
iii) earthquake hypocentre depth distribution,
iv) upper and lower seismogenic depths, and
v) distribution of rupture nodal plane properties (strike, dip, rake).

Hence, such regionalization can be extracted from one of the seismogenic sources of ESHM20 (Danciu et al., 2021; 2022), such as the area source model. The following rupture parameters are given in the ESHM20:

- three values of hypocentral depth and their corresponding weights
- four values for the dip and strike angle
- three styles of faulting (i.e., normal, reverse and strike-slip) from which the rake values can be also assigned
- upper and lower seismogenic depths
- magnitude to rupture area scaling relation (Leonard, 2014)

Figure 10 illustrates the regional distribution of the average hypocenter depth derived from the area source model of ESHM20, whereas Figure 11 shows the spatial distribution of one set of values for the dip and strike angles, the parameters that define the nodal plane of the rupture.

With this information, the point-earthquakes contained in, for example, ETAS-generated synthetic catalogues can be spatially linked with seismic sources and the source-specific rupture parameters can be attributed to the earthquakes. (Papadopoulos, Bazzurro, and Marzocchi 2021).

Following the definition of the finite ruptures, the generation of ground motion fields for OEF is no different from any other seismic hazard or risk modelling application, and requires the following ground motion components:

- selection of a ground motion model (GMM) or a set of ground motion models combined by means of a logic tree;
- consideration of spatial and inter-period correlation of the variability;
- model of aleatory uncertainties (distinguish between the inter- and intra-event)
- definition of a site model to characterise soil conditions.

Some researchers have noted systematic differences in the median spectral accelerations of mainshock and aftershock events of comparable magnitude (Abrahamson et al. 2008; Baltay and Hanks 2013; Boore and Atkinson 1989; Chiou and Youngs 2008). As a result, an additional "aftershock" term is often used in certain GMPE models to scale the median ground motions of aftershock accordingly (e.g. Abrahamson, Silva, and Kamai 2014; Chiou and Youngs 2008).

Abrahamson et al. (2014) apply this scaling term only to aftershocks occurring within a certain distance to the mainshock, i.e. practically assuming that ground motions of events triggered at further distances would have no material differences to those of mainshocks (of comparable magnitude). Moreover, Papadopoulos et al. (2019) have demonstrated that the ground motion residuals of mainshock-aftershock pairs are mildly interconnected. Such ground motion correlations could reflect similarities in source-, path- and site-effects. Capturing such effects by modelling the correlation of sequential ground motions could have a measurable impact on hazard and loss probabilities. These similarities might also be captured in part by using site-constrained non-ergodic ground motion models, which would reduce uncertainty and perhaps eliminate some of the observed correlations.

Additional complexity associated to the simulated ground motion fields are for example, the multi-fault ruptures, directivity, hanging-wall effects, basin effects and nonlinearity in the ground motion models (Field, 2022). Further research should seek to provide further insights on the best-practices for modelling ground motions within an OEF framework.

At the European level, the ground motion logic tree (Weatherill et al., 2021) used in ESHM20 (Danciu et al., 2021) might be used for modelling the ground motion fields of the generated earthquake catalogue. The ground motion logic tree covers both the epistemic and the aleatory uncertainties, and are implemented in OpenQuake (Pagani et al 2014). Furthermore, the site model (Weatherill et al., 2022) provides the basis for the site amplification layer for risk assessment, as briefly described in the next section.

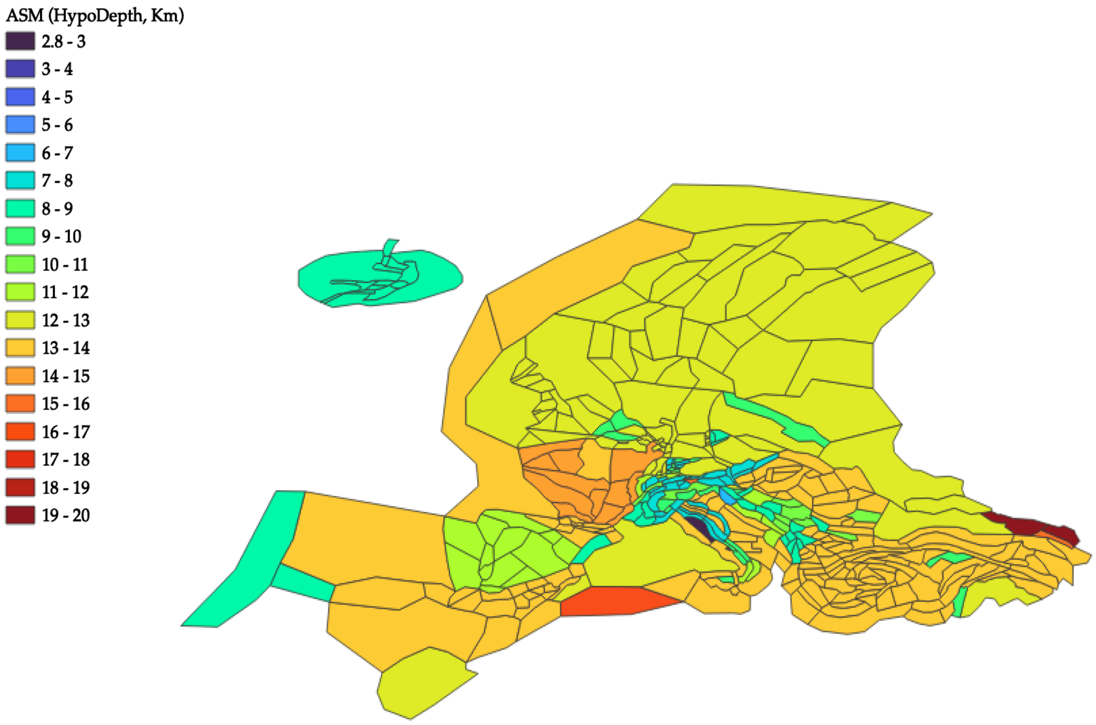

F

Fig. 13 The spatial distribution of the average hypocentre depth from the ESHM20 area source model (Danciu et al., 2021)

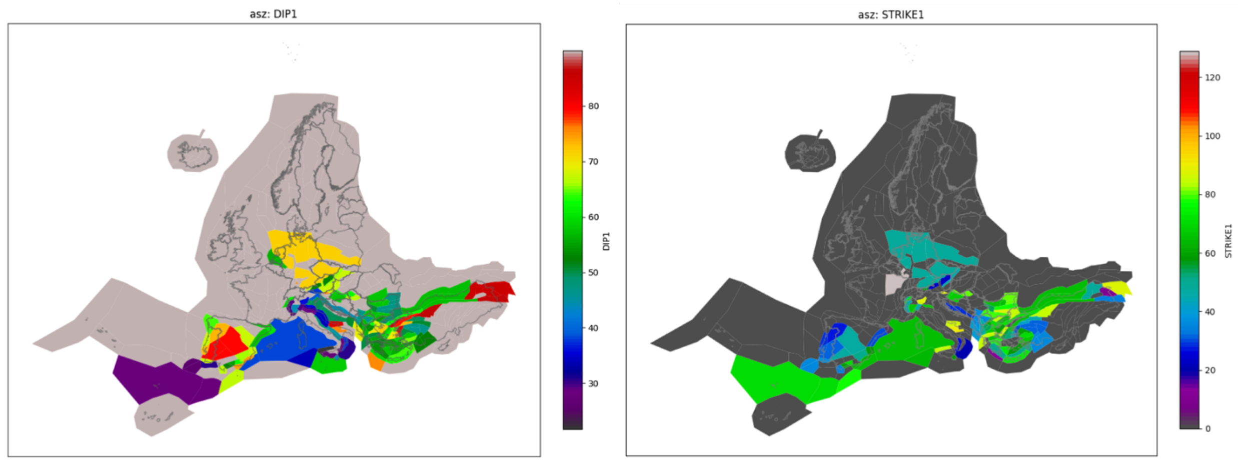

Fig. 14 Spatial distribution of dip and strike angles associated with the ESHM20 area source model (Danciu et al., 2021). Note that four values are assigned to these two parameters, though only one is illustrated here.

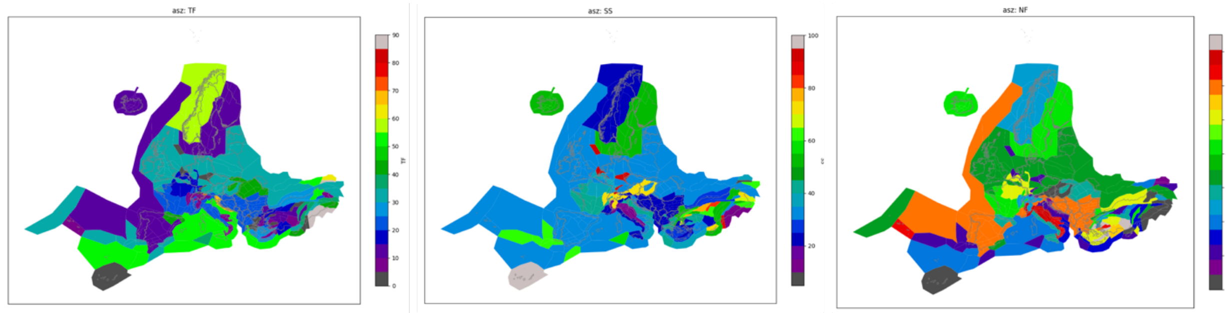

Fig. 15 Spatial distribution of the predominant style-of-faulting i.e. thrust (left), normal (middle) and strike-slip (right) associated with the area source model of ESHM20 (Danciu et al., 2021)

4.3 A European OEF Model – Damage and Loss Assessment

The feasibility of establishing Operational Earthquake Loss Forecasting (OELF) at the European scale will depend on the ongoing developments described in the previous sections. Hence, this is not yet a service that has been developed in the RISE project, but other RISE deliverables, namely Deliverable 4.3 and Deliverable 6.2 have demonstrated OELF systems at the national scale through the MANTIS-K and MANTIS v2.0 systems that has been set up in Italy.

Once there is a system that can generate OEF rates (Section 4.1), and then estimate for any location in Europe the associated ruptures and levels of ground shaking (Section 4.2), it will be fairly straightforward to assess losses in a European OELF system with the exposure and vulnerability models described for the European Rapid earthquake Loss Assessment (RLA) tool in Section 2.2.

However, this would assume that damage does not accumulate and affect the fragility of buildings to subsequent earthquakes, and that the occupancy of the buildings is constant and independent of time. Deliverable 6.1 has run a number of case studies which demonstrate the impact of damage dependence and time variance of exposure models within OELF.

The methodology and open-source tools are therefore available to the research community to investigate these phenomena further. What is needed for a European-wide system that incorporates the dynamics of vulnerability and exposure would be a set of damage-dependent fragility functions to be developed for the European building stock, and for additional models on the post-event occupancy of buildings to be proposed (also using empirical data) and tested.

5. References

Abrahamson, N., Silva W.J, and Kamai R. 2014. "Summary of the ASK14 Ground Motion Relation for Active Crustal Regions." Earthquake Spectra 30(3):1025–55.

Abrahamson, N., Atkinson G., Boore D., Bozorgnia Y., Campbell K., Chiou B., Idriss I.M., Silva W., and Youngs R. 2008. "Comparisons of the NGA Ground-Motion Relations." Earthquake Spectra 24(1):45–66.

Baltay, A. and Hanks T.C. 2013. "Understanding the Magnitude Dependence of PGA and PGV: A Look at Differences between Mainshocks and Aftershocks in the NGA-West2 Data and Ground Motion from Small Magnitude Anza Data." in Proceedings of the American Geophysical Union Fall Meeting. San Francisco, CA.

Boore, D.M. and Atkinson G.M. 1989. "Spectral Scaling of the 1985 to 1988 Nahanni, Northwest Territories, Earthquakes." Bulletin of the Seismological Society of America 79(6):1736–61.

Bossu, R., Finazzi, F., Steed, R., Fallou, L. and Bondár, I., 2022. "Shaking in 5 Seconds!"—Performance and user appreciation assessment of the earthquake network smartphone-based public earthquake early warning system. Seismological Research Letters, 93(1), pp.137-148.

Bossu, R., Roussel, F., Fallou, L., Landès, M., Steed, R., Mazet-Roux, G., ... & Petersen, L. (2018). LastQuake: From rapid information to global seismic risk reduction. International journal of disaster risk reduction, 28, 32-42.

Chiou, B.. and Youngs R. 2008. "An NGA Model for the Average Horizontal Component of Peak Ground Motion and Response Spectra." Earthquake Spectra 24(1):173–215.

Christophersen, A, D. Rhoades, M Gerstenberger, Stephen Bannister, Julia Becker, Sally Potter, and Sara McBride. 2017. "Progress and Challenges in Operational Earthquake Forecasting in New Zealand 2017 NZSEE Conference." In .

Crowley H., Dabbeek J., Despotaki V., Rodrigues D., Martins L., Silva V., Romão, X., Pereira N., Weatherill G. and Danciu L. (2021) European Seismic Risk Model (ESRM20), EFEHR Technical Report 002, V1.0.1, 84 pp, https://doi.org/10.7414/EUC-EFEHR-TR002-ESRM20

Dabbeek J., Crowley H., Silva V., Weatherill G., Paul N., Nievas C. (2021) "Impact of exposure spatial resolution on seismic loss estimates in regional portfolios," Bulletin of Earthquake Engineering, 19 (14), pp. 5819-5841

Danciu L, Nandan S, Reyes C, Basili R, Weatherill G, Beauval C, Rovida A, Vilanova S, Sesetyan K, Bard P-Y, Cotton F, Wiemer S, Giardini D (2021) The 2020 update of the European Seismic Hazard Model – ESHM20: Model Overview. EFEHR Technical Report 001 v1.0.0. https://doi.org/10.12686/a15

Danciu, Laurentiu, Graeme Weatherill, Andrea Rovida, Roberto Basili, Pierre-Yves Bard, Céline Beauval, Shyam Nandan, et al. 2022. "The 2020 European Seismic Hazard Model: Milestones and Lessons Learned." In Progresses in European Earthquake Engineering and Seismology, edited by Radu Vacareanu and Constantin Ionescu, 3–25. Springer Proceedings in Earth and Environmental Sciences. Cham: Springer International Publishing. https://doi.org/10.1007/978-3-031-15104-0_1.

Earle P.S., Wald D.J., Jaiswal K.S., Allen T.I, Hearne M.G., Marano K.D., Hotovec A.J., and Fee J. (2009) Prompt Assessment of Global Earthquakes for Response (PAGER): A System for Rapidly Determining the Impact of Earthquakes World-wide U.S. Geological Survey Open-File Report, no. 2009–1131, https://doi.org/10.3133/ofr20091131.

Earthquake Forecasting Models for Switzerland." In preparation.

Engler, D. T., C. B. Worden, E. M. Thompson, K. S. Jaiswal (2022). Partitioning Ground Motion Uncertainty When Conditioned on Station Data. Bull. Seism. Soc. Am. 2022; doi: https://doi.org/10.1785/0120210177

Fallou, L., Finazzi, F. and Bossu, R., 2022. Efficacy and Usefulness of an Independent Public Earthquake Early Warning System: A Case Study—The Earthquake Network Initiative in Peru. Seismological Society of America, 93(4), pp.2410-2410.

FEMA [2003] ''HAZUS-MH Technical Manual,'' Federal Emergency Management Agency, Washington D.C.

Edward H. Field; Some Systemic Risks to Progress on Seismic Hazard Assessment. Seismological Research Letters 2021;; 93 (2A): 513–516. doi: https://doi.org/10.1785/0220210268

Field, Edward H., Kevin R. Milner, Jeanne L. Hardebeck, Morgan T. Page, Nicholas van der Elst, Thomas H. Jordan, Andrew J. Michael, Bruce E. Shaw, and Maximilian J. Werner. 2017. "A Spatiotemporal Clustering Model for the Third Uniform California Earthquake Rupture Forecast (UCERF3-ETAS): Toward an Operational Earthquake Forecast." Bulletin of the Seismological Society of America 107 (3): 1049–81.

Finazzi, F., Bondár, I., Bossu, R. and Steed, R., 2022. A Probabilistic Framework for Modeling the Detection Capability of Smartphone Networks in Earthquake Early Warning. Seismological Society of America, 93(6), pp.3291-3307.

for Europe" In preparation.

github. "GitHub," 2020. https://github.com/.

Grünthal, G. (Ed.) (1998) European Macroseismic Scale 1998 (EMS-98) European Seismological Commission, sub commission on Engineering Seismology, Working Group Macroseismic Scales. Conseil de l'Europe, Cahiers du Centre Européen de Géodynamique et de Séismologie, Vol. 15, Luxembourg.

Guo, Y., Zhuang J., and Zhou S. 2015. "A Hypocentral Version of the Space-Time ETAS Model." Geophysical Journal International 203(1):366–72.

Han, Marta, Leila Mizrahi, Stefan Wiemer. 2023. "Towards Operational Earthquake Fore-casting

Jaiswal K. and Wald D. (2013) "Estimating Economic Losses from Earthquakes Using an Empirical Approach," Earthquake Spectra, 29(1), pp. 309-324.

Jaiswal K., Wald D. and Hearne M. (2009) Estimating casualties for large worldwide earthquakes using an empirical approach, US Geological Survey Open-File Report 1136.

Jaiswal K.S. and Wald D.J. (2008) Creating a global building inventory for earthquake loss assessment and risk management, US Geological Survey Open-File Report 1160.

Jordan, T. H., W. Marzocchi, A. J. Michael, and M. C. Gerstenberger. 2014. "Operational Earthquake Forecasting Can Enhance Earthquake Preparedness." Seismological Re-search Letters 85 (5): 955–59. https://doi.org/10.1785/0220140143.

Jordan, T., Y.-T. Chen, Paolo Gasparini, Raul Madariaga, Ian Main, Warner Marzocchi, Gerassimos Papadopoulos, K. Yamaoka, and J. Zschau. 2011. "Operational Earth-quake Forecasting: State of Knowledge and Guidelines for Implementation." Annals of Geophysics.

Jozinović, Dario, Valentino Lauciani, Sergio Bruni, Licia Faenza, and Alberto Michelini. "ShakeMap4-Web: Web Application for ShakeMap 4 Product Visualization." Seismological Research Letters, October 12, 2022. https://doi.org/10.1785/0220220082.

Leonard, M. (2014). Self-Consistent Earthquake Fault-Scaling Relations: Update and Extension to Stable Continental Strike-Slip Faults. Bulletin of the Seismological Society of America, 104(6), 2953–2965. https://doi.org/10.1785/0120140087

Marzocchi, Warner, and Anna Maria Lombardi. 2009. "Real-Time Forecasting Following a Damaging Earthquake." Geophysical Research Letters 36 (21).

Marzocchi, Warner, Anna Maria Lombardi, and Emanuele Casarotti. 2014. "The Establishment of an Operational Earthquake Forecasting System in Italy." Seismological Re-search Letters 85 (5): 961–69.

Merkel, Dirk. "Docker: Lightweight Linux Containers for Consistent Development and Deployment." Linux Journal 2014, no. 239 (2014): 2.

Mizrahi Leila, Nicolas Schmid, & Marta Han. (2023). lmizrahi/etas: ETAS with fit visualization (3.2). Zenodo. https://doi.org/10.5281/zenodo.7584575

Mizrahi, Leila, Shyam Nandan, and Stefan Wiemer. 2021. "Embracing Data Incompleteness for Better Earthquake Forecasting." Journal of Geophysical Research: Solid Earth 126 (12): e2021JB022379.

Mizrahi, Leila, Shyam Nandan, Stefan Wiemer. 2023. "Developing and Testing ETAS-Based

Ogata, Yosihiko. 1988. "Statistical Models for Earthquake Occurrences and Residual Analysis for Point Processes." Journal of the American Statistical Association 83 (401): 9–27. https://doi.org/10.1080/01621459.1988.10478560.

Papadopoulos, A.N., Kohrangi M., and Bazzurro P. (2019). "Correlation of Spectral Acceleration Values of Mainshock-Aftershock Ground Motion Pairs." Earthquake Spectra 35(1):39–60.

Papadopoulos, A.N., Bazzurro P., and Marzocchi W. 2021. "Exploring Probabilistic Seismic Risk Assessment Accounting for Seismicity Clustering and Damage Accumulation: Part I. Hazard Analysis." Earthquake Spectra 37(2):803–26.

Pittore M., Wieland M., Errize M., Kariptas C., Gungor I. (2015) "Improving Post-Earthquake Insurance Claim Management: A Novel Approach to Prioritize Geospatial Data Collection," International Journal of Geo-Information, 4(4), pp. 2401-2427; https://doi.org/10.3390/ijgi4042401

Quitoriano, V. & Wald, D. J. (2022) Combining Macroseismic Intensity Felt Reports Using ShakeMap. Proceedings of the 3rd European Conference on Earthquake Engineering and Seismology. Bucharest

Rhoades, David A., Danijel Schorlemmer, Matthew C. Gerstenberger, Annemarie Christophersen, J. Douglas Zechar, and Masajiro Imoto. 2011. "Efficient Testing of Earthquake Forecasting Models." Acta Geophysica 59 (4): 728–47. https://doi.org/10.2478/s11600-011-0013-5.

Savran, William, Maximilian Werner, Danijel Schorlemmer, and Philip Maechling. 2022. "PyCSEP: A Python Toolkit For Earthquake Forecast Developers." Journal of Open Source Software 7 (69): 3658. https://doi.org/10.21105/joss.03658.

Schorlemmer, D., M. C. Gerstenberger, S. Wiemer, D. D. Jackson, and D. A. Rhoades. 2007. "Earthquake Likelihood Model Testing." Seismological Research Letters 78 (1): 17–29. https://doi.org/10.1785/gssrl.78.1.17.

Wald D. J., Quitoriano V., Heaton T.H., Kanamori H., Scrivner C.W. and Worden C.B. (1999) "TriNet "ShakeMaps": Rapid Generation of Peak Ground Motion and Intensity Maps for Earthquakes in Southern California," Earthquake Spectra, 15(3), pp. 537–555.

Wald DJ, Jaiswal KS, Marano KD, Bausch D. (2010) An Earthquake Impact Scale, Natural Hazards Review, 12, 125-139

Wald DJ, Marano KD, Jaiswal KS, Thompson E, James-Ravenell M and Hearne M. (2022) Evaluating a decade of U.S. Geological Survey's PAGER Real-Time Earthquake Loss Estimates, 12th National Conference on Earthquake Engineering, Salt Late City, Utah.

Wald, D. J., Quitoriano, V., Worden, C. B., Hopper, M., & Dewey, J. W. (2011). USGS "Did You Feel It?" internet-based macroseismic intensity maps. Ann. Geophys., 54(6), 688.

Weatherill G, Crowley H, Roullé A, Tourlière B, Lemoine A, Gracianne C, Kotha SR, Cotton F (2022) Modelling site response at regional scale for the 2020 European Seismic Risk Model (ESRM20). Bulletin of Earthquake Engineering 21:665-714. https://doi.org/10.1007/s10518-022-01526-5

Worden C.B., Thompson E. M., Hearne M. and Wald D.J. (2020) ShakeMap Manual Online: Technical Manual, User's Guide, and Software Guide, https://doi.org/10.5066/F7D21VPQ. http://usgs.github.io/shakemap/.

Zechar, J. D., M. C. Gerstenberger, and D. A. Rhoades. 2010. "Likelihood-Based Tests for Evaluating Space-Rate-Magnitude Earthquake Forecasts." Bulletin of the Seismolog-ical Society of America 100 (3): 1184–95. https://doi.org/10.1785/0120090192.

RISE Deliverables

Deliverable 4.3, Chioccarelli et al. (2022) "Operational earthquake loss forecasting for Europe"

Deliverable 5.9, Finazzi et al. (2023) "Crowdsourced EEW services"

Deliverable 6.1, Nievas et al. (2023) "Integration of RISE innovations in the fields of OELF, RLA and SHM"

Deliverable 6.2, Chioccarelli et al. (2023) "Report on testing OEF and extending earthquake forecasts to loss forecasts in Italy"